

CHEMISTRY

AN **ASIAN** JOURNAL

www.chemasianj.org

Accepted Article

Title: Triphenylamine-appended half-sandwich iridium(III) complexes and their biological applications

Authors: Zhe Liu, Xiangdong He, Meng Tian, Xicheng Liu, Yanhua Tang, Changfang Shao, Peiwei Gong, Jinfeng Liu, Shumiao Zhang, and Lihua Guo

This manuscript has been accepted after peer review and appears as an Accepted Article online prior to editing, proofing, and formal publication of the final Version of Record (VoR). This work is currently citable by using the Digital Object Identifier (DOI) given below. The VoR will be published online in Early View as soon as possible and may be different to this Accepted Article as a result of editing. Readers should obtain the VoR from the journal website shown below when it is published to ensure accuracy of information. The authors are responsible for the content of this Accepted Article.

To be cited as: *Chem. Asian J.* 10.1002/asia.201800103

Link to VoR: <http://dx.doi.org/10.1002/asia.201800103>

A Journal of



A sister journal of *Angewandte Chemie* and *Chemistry – A European Journal*

WILEY-VCH

Triphenylamine-appended half-sandwich iridium^{III} complexes and their biological applications

Xiangdong He^{a,†}, Meng Tian^{a,†}, Xicheng Liu^{a,*}, Yanhua Tang^a, Changfang Shao^a, Peiwei Gong^a, Jinfeng Liu^b, Shumiao Zhang^a, Lihua Guo^a, Zhe Liu^{a,*}

^a Institute of Anticancer Agents Development and Theranostic Application, The Key Laboratory of Life-Organic Analysis and Key Laboratory of Pharmaceutical Intermediates and Analysis of Natural Medicine, Department of Chemistry and Chemical Engineering, Qufu Normal University, Qufu 273165, China.

^b Qufu Normal University, School of Life Science, Qufu 273165, China.

* Corresponding author: E-mail: chemlxc@163.com (Xicheng Liu); liuzheqd@163.com (Zhe Liu).

[†] X. D. He and M. Tian have equivalent contribution

Abstract: Organometallic half-sandwich Ir^{III} complexes of type $[(\eta^5\text{-Cp}^x)\text{Ir}(\text{N}^{\wedge}\text{N})\text{Cl}]\text{PF}_6$ (Cp^x: Cp* or its phenyl Cp^{xph} or biphenyl Cp^{xbiph} derivatives, N[∧]N: triphenylamine (TPA) substituted bipyridyl ligand groups) have been synthesized and characterized. The complexes showed excellent BSA and DNA binding properties, and oxidize NADH to NAD⁺ efficiently. Complexes can induce apoptosis effectively and led to the emergence of reactive oxygen species (ROS) in cells. All complexes showed potent cytotoxicity with IC₅₀ values ranging from 1.5 to 7.1 μM toward A549 human lung cancer cells after 24 h drug exposure, at most 14 times more potent than *cis*-platin under the same conditions.

INTRODUCTION

The clinical success and drawbacks of Pt anticancer drugs have stimulated the exploration of other metal-based anticancer complexes.^[1] Recently, iridium^{III} (Ir^{III}) complexes have attracted much attention because of their wide biological applications.^[2-11] Ir^{III} complexes are often viewed as relatively inert, a common characteristic of low-spin d^6 metal ions and especially third-row transition metals.^[12] However, Ir^{III} complexes have shown potent anticancer activity,^[2,13-15] and displayed a different mechanism of action (MoA) compared with conventional platinum-based drugs.^[16,17]

Due to the advantages of high anticancer activity and unique MoA, half-sandwich organometallic Ir^{III} complexes have attracted extensive interest.^[18-20] In a recent study, Sadler and coworkers found that half-sandwich Cp* (pentamethylcyclopentadienyl) Ir^{III} complexes with *N,N*-bound ligand, such as 2,2'-bipyridine (bipy), 1,10-phenanthroline (phen) and ethylenediamine (EDA), were all inactive against A2780 human ovarian cancer cells with IC₅₀ values

(concentrations at which 50% of the cell growth is inhibited) over 100 μM .^[21,22] The increase of benzene rings on the Cp ring has a great effect on the anticancer activity of the complexes. It is noteworthy that the electronic and steric properties of the ligands have a major effect on the chemical and biological activities to Ir^{III} complexes.^[23,24] Other work also proved that replacing the chelating ligands has significant effect on changing the lipid solubility of the complexes and can improve antitumor activity significantly.^[25] This encouraged us to explore the activity of complexes containing bipy derivatives in more details.

Triphenylamine (TPA) is a promising organic functional material in organic photoelectric field, however, its biological application is rare. In this study, six half-sandwich complexes of the type $[(\eta^5\text{-Cp}^x)\text{Ir}(\text{N}^x\text{N})\text{Cl}]\text{PF}_6$ (**Figure 1**) have been synthesized and characterized, where (Cp^*) is phenyl derivatives (Cp^{xph}), biphenyl derivatives (Cp^{xbiph}), and the N^xN -chelating ligands are bipy linked with TPA groups through double bond, which can enhance the lipid solubility of Ir^{III} complexes, accordingly enhancing anticancer activity. The six Ir^{III} complexes display higher antitumor activity against A549 lung cancer cells (1.5 ~7.1 μM) than *cis*-platin (21.3 μM) under the same conditions. Furthermore, all complexes can bind with BSA and DNA and oxidize NADH to NAD^+ . Ir^{III} complexes can effectively induce apoptosis and promoting the production of reactive oxygen species (ROS) in cells. The results suggest that triphenylamine-appended half-sandwich Ir^{III} complexes are hopeful for development as new anticancer agents.

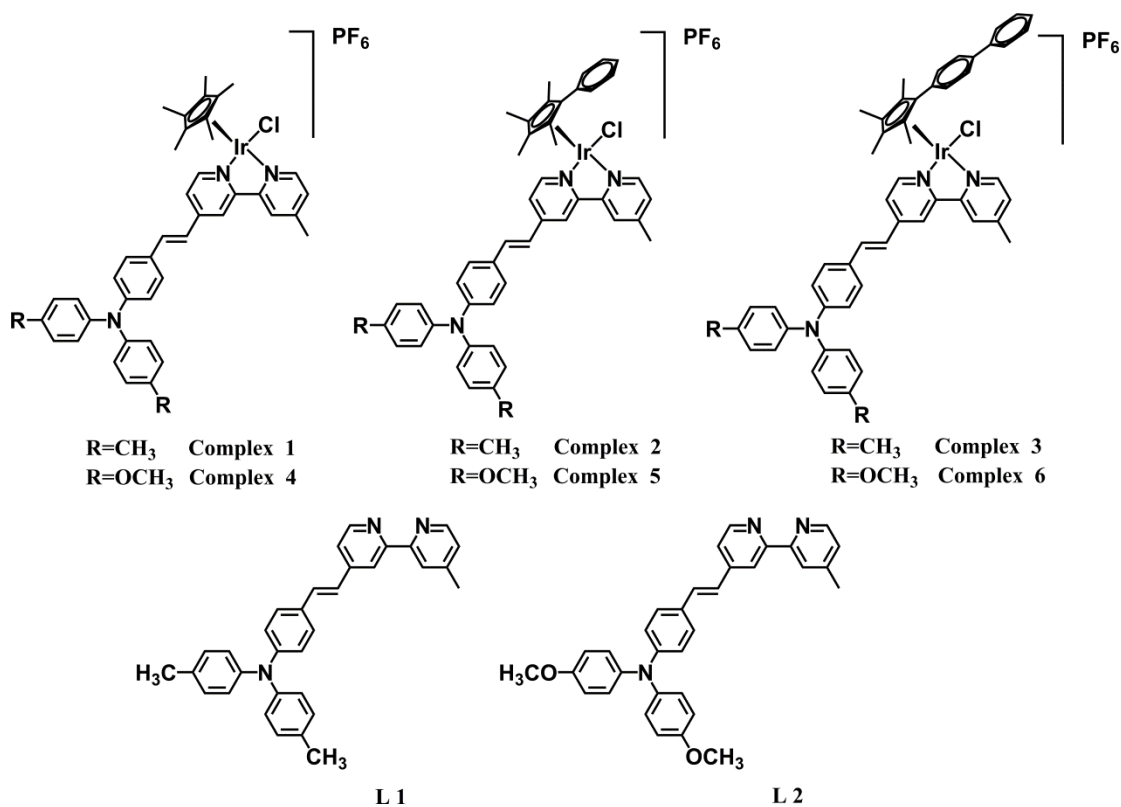
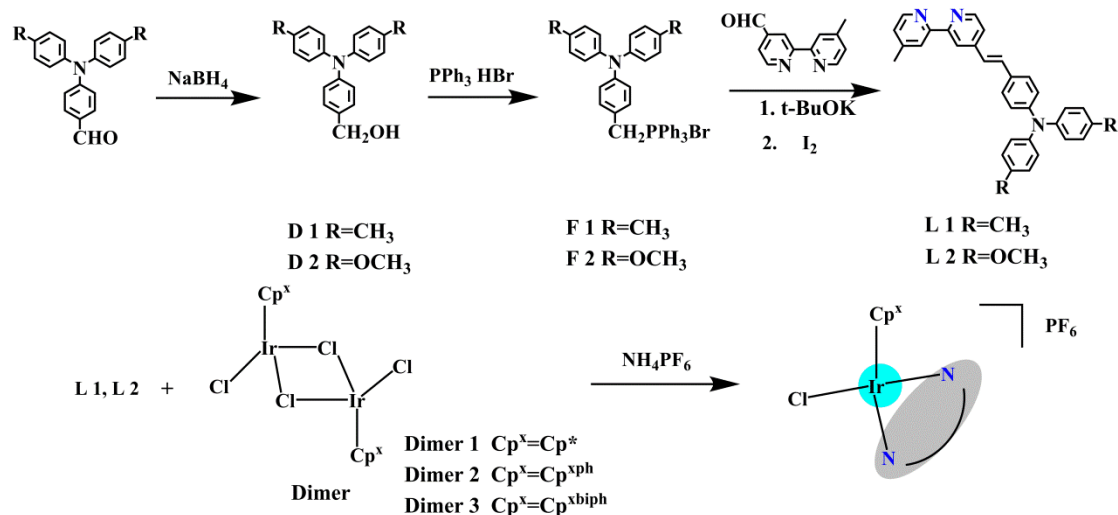


Figure 1 The structure of as-synthesized half-sandwich organometallic Ir^{III} complexes.

Results and Discussion

Ir^{III} half-sandwich complexes of the type $[(\eta^5\text{-Cp}^x)\text{Ir}(\text{N}^{\wedge}\text{N})\text{Cl}]\text{PF}_6$ were synthesized in methanol at ambient temperature, and the N[∧]N-chelating ligands were synthesized by Wittig reaction and got the *trans* structure by reflux with a catalytic amount of iodine. All complexes are new synthesized complexes and obtained in good yields. Synthesis processes are shown in **Scheme 1**. Ir^{III} complexes and the intermediates were characterized by ¹H NMR and mass spectroscopy. All Ir^{III} complexes were isolated as PF₆⁻ salts.



Scheme 1 Synthesis process of Ir^{III} complexes.

2.1 Cytotoxicity test

The antitumor activity of as-synthesized complexes against A549 human lung cancer cell have been determined by MTT assay, the IC₅₀ values after exposure to six complexes and *cis*-platin for 24h are listed in **Table 1**. Notably, compared to *cis*-platin, as-synthesized six complexes have better antitumor activity against A549 lung cancer cells with IC₅₀ values range from 1.5 to 7.1 μM. However, there is no better selectivity for the normal cell line 16HBE (human bronchial epithelial cells) and BEAS-2B (human bronchial epithelial cells) for the complexes (**Table S1**). As shown, complexes containing Cp^{xph} ligand (complexes **2** and **5**) showed higher antiproliferative activity compare to their Cp* analogues (complexes **1** and **4**), probably due to the enhanced lipid solubility caused by the Cp^{xph} ligand. However, introduction of the larger Cp^{xbiph} ligand in complexes **3** and **6** led to lower antiproliferative activity, probably due to the high hydrophobicity of the chelating ligand. Therefore, the Cp^{xph} ligand based complexes showed the best anticancer activity. Sadler and coworkers have confirmed that Cp* Ir^{III} complexes with 2,2'-bipyridine (bipy) are inactive against A2780 human ovarian cancer cells with IC₅₀ values over 100 μM.^[21,22] Therefore, the introduction of TPA group into bipy ligand played a crucial role to switch on the anticancer activity of the complexes. However, variation of terminal groups (methyl and methoxyl) on TPA group has less effect on the anticancer activity.

The cytotoxic activity of two ligands L1 and L2 was also tested, which showed no anticancer activity, **Table 1**. In addition, the iridium dimers displayed inactivity or medium anti-cancer

activity.^[18] Interestingly, the complexes formed by coordination of iridium and TPA ligand possessed high potency.

Table 1 Inhibition of growth toward A549 lung cancer cells by complexes **1–6** and comparison with *cis*-platin recorded over a period of 24 h.

Complex	IC ₅₀ (μM) A549
$[(\eta^5\text{-C}_5\text{Me}_5)\text{Ir}(\text{L}_1)\text{Cl}]\text{PF}_6$ (1)	6.8 ± 0.5
$[(\eta^5\text{-C}_5\text{Me}_4\text{C}_6\text{H}_5)\text{Ir}(\text{L}_1)\text{Cl}]\text{PF}_6$ (2)	1.5 ± 0.1
$[(\eta^5\text{-C}_5\text{Me}_4\text{C}_6\text{H}_4\text{C}_6\text{H}_5)\text{Ir}(\text{L}_1)\text{Cl}]\text{PF}_6$ (3)	3.6 ± 0.5
$[(\eta^5\text{-C}_5\text{Me}_5)\text{Ir}(\text{L}_2)\text{Cl}]\text{PF}_6$ (4)	4.8 ± 2.1
$[(\eta^5\text{-C}_5\text{Me}_4\text{C}_6\text{H}_5)\text{Ir}(\text{L}_2)\text{Cl}]\text{PF}_6$ (5)	1.7 ± 0.2
$[(\eta^5\text{-C}_5\text{Me}_4\text{C}_6\text{H}_4\text{C}_6\text{H}_5)\text{Ir}(\text{L}_2)\text{Cl}]\text{PF}_6$ (6)	7.1 ± 0.8
<i>Cis</i> -platin	21.3 ± 1.7
L1	>100
L2	>100

2.2 Reaction with NADH

In many biological processes, coenzyme NADH play a major role.^[15] Ir^{III} cyclopentadienyl complexes can oxidize NADH to generate reactive oxygen species (ROS) H₂O₂, which provide a pathway to a mechanism of oxidant.^[26,27] The interaction of as-synthesized complexes with NADH can be detected by measuring the maximum absorbance at 259 nm and 340 nm over time with an ultraviolet-visible (UV-Vis) spectrophotometer (**Figure 2** and **Figure S1** in supporting information). Among these, the peaks at short wavelength (~259 nm) can be assigned to the absorption of NAD⁺ (The complexes capture hydrogen ions on NADH to produce NAD⁺), while peaks at longer wavelength (~340 nm) are the absorption of NADH.^[27] The turnover numbers (TONs) of complexes **1** (42.4), **2** (27.5) **3** (2.1) **4** (31.3) **5** (14.4) and **6** (13.9) was calculated by measuring the difference at 339 nm (**Figure 2b**). With the increase of the number of benzene rings in Cp rings, the TONs of complexes decreased gradually. This phenomenon is attributed to the increase of the benzene ring in the Cp ring, which increases the steric hindrance of the complexes and decreases the ability of the complexes to oxidize NADH.

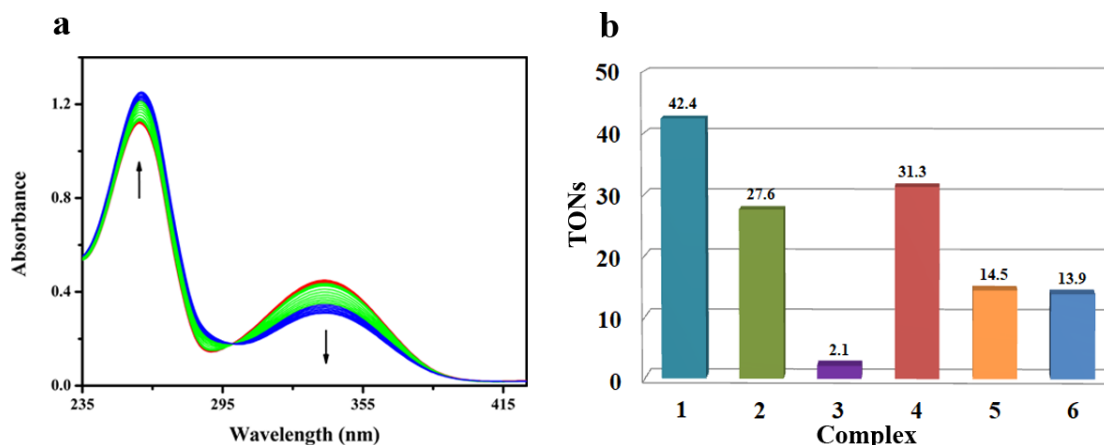


Figure 2 (a) UV-Vis spectra of the reaction of NADH (100 μM) with complex 4 (1 μM) in 10% MeOH/90% H_2O (V:V) at 298 K for 8 h; (b) The TONs of as-synthesized complexes. The arrows show changes in absorbance spectra over time.

2.3 Study of BSA interactions

Investigating the interaction between anticancer agents and protein is conducive to understand what happened in cells.^[28] Serum albumin (SA) is the main protein which play an important role in drug transport and metabolism in blood plasma.^[29] In this study, because of the similar to human serum albumin (HSA) in structure and easily obtained, bovine serum albumin (BSA) was used to test the binding to complexes by investigated the quenching of BSA. If the quenching mechanism is a static quenching mechanism, changes in the absorption intensity (278nm) are accompanied by significant wavelength shifts, while the dynamic quenching is without any wavelength shifts.^[12] From **Figure 3a**, we can see that there is no wavelength shift in 278 nm after adding complexes 1~6 to BSA solution, which indicate the interaction between BSA and complexes is in the form of dynamic quenching.^[30]

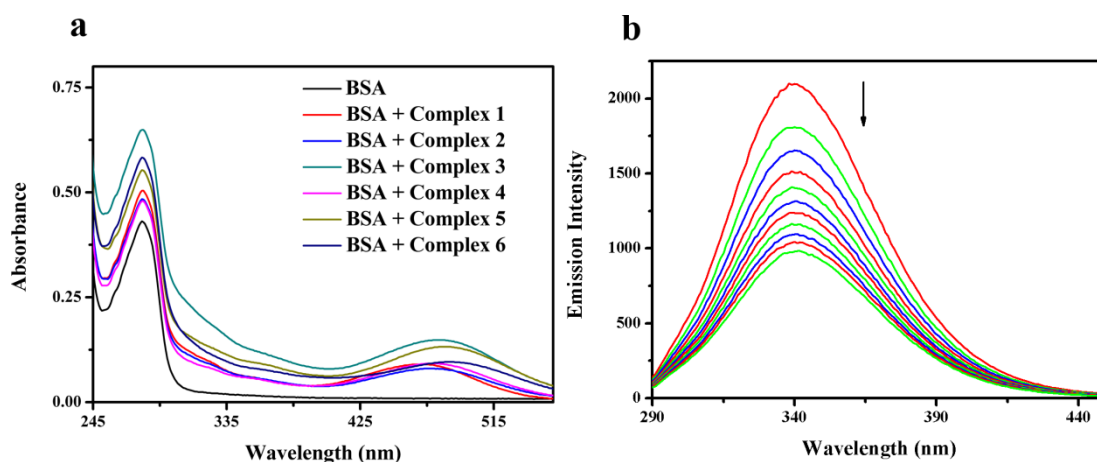


Figure 3 (a) UV-Vis spectrum of BSA (10 μM) in 5 mM Tris-HCl/50 mM NaCl buffer solution (pH = 7.2) upon addition of the complexes 1-6 (5 μM). (b) Fluorescence spectra of BSA (10 μM ;

$\lambda_{\text{ex}} = 280 \text{ nm}$; $\lambda_{\text{em}} = 343 \text{ nm}$) in the absence and presence of complex **3** (0–10 μM). The arrows show changes in absorbance spectrum of BSA upon increasing the amounts of complexes **3**.

Fluorescence quenching is another effective method to study the interaction between complexes and proteins. As shown in **Figure 3b** (**Figure S2** in supporting information), with the increase of complex **3**, the fluorescence intensity of BSA (10 μM) at 343 nm decreases continuously.^[31-35] To get a possible quenching mechanism, emission quenching data have been analyzed by the classical Stern–Volmer equation and Scatchard equation.^[12,36-39] As shown in **Table 2**, the Stern–Volmer quenching constant K_{sv} and the quenching rate constant K_q and the binding site number n of all complexes have no obvious change law, but the value of the binding constant K_b will increase with the increase of the number of benzene rings on the Cp ring: $\text{Cp}^* > \text{Cp}^{\text{Xph}} > \text{Cp}^{\text{Xbiph}}$. This result indicate that the introduction of benzene ring and diphenyl ring in Cp have an adverse effect on the complexes binding to BSA. This is mainly due to the increasing steric hindrance with the introduction of benzene ring and diphenyl ring on Cp, thereby affecting the binding of complexes to BSA.

Table 2 The values of K_{sv} , K_b and K_q for as-synthesized complexes.

Complex	K_q ($10^{13} \text{ M}^{-1}\text{S}^{-1}$)	K_{sv} (10^5 M^{-1})	K_b (10^4 M^{-1})	n
1	1.17	1.17±0.16	22.56	1.05
2	0.77	0.77±0.15	6.08	0.98
3	1.24	1.24±0.15	2.33	0.87
4	1.05	1.05±0.18	10.08	1.00
5	1.11	1.11±0.16	6.51	0.96
6	1.39	1.39±0.14	3.71	0.91

Synchronous fluorescence spectra were obtained by a similar method to study the microenvironment in the vicinity of the fluorophore.^[40] The effect of the complexes **3** and **6** in the BSA are shown in **Figure 4** (**Figure S5** and **S6** in supporting information). With the increase of complexes **3** and **6**, both the synchronous fluorescence spectra for BSA markedly reduce in fluorescence intensity at 283 and 275 nm ($\Delta\lambda$: 15 nm and 60 nm, which are the characteristic of synchronous emission spectrum for tyrosine and tryptophan residue, respectively^[41]). The synchronous fluorescence spectrum has a displacement of 2-3 nm at $\Delta\lambda = 15 \text{ nm}$, while no

wavelength shift at $\Delta\lambda = 60$ nm, which indicating as-synthesized complexes mainly changes the microenvironment of tyrosine for BSA.

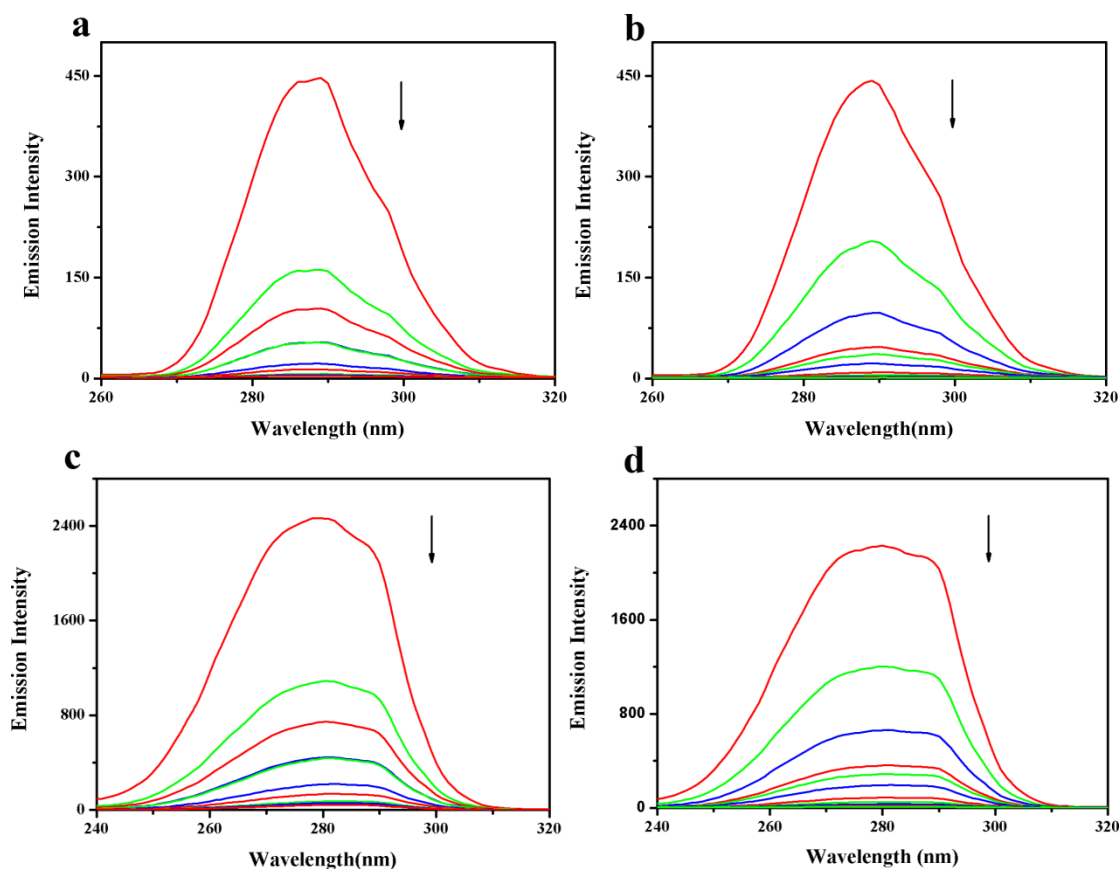


Figure 4 Synchronous spectra of BSA (20 μ M) with complexes **3** and **6**, increasing (0–50 μ M) with a wavelength difference of [(a) **3**, (b) **6**] $\Delta\lambda = 15$ nm and [(c) **3**, (d) **6**] $\Delta\lambda = 60$ nm. The arrows show changes in emission intensity of BSA upon increasing the amounts of complexes **3** and **6**.

2.4 Interaction with CT-DNA

The interaction of base pairs of DNA with complexes usually involves intercalation, interaction, non-intercalative, electrostatic interactions and damage of the DNA double helix.^[42-45] Change of the absorption wavelength of the as-synthesized complexes with increasing of CT-DNA (DNA sodium from calf thymus) was achieved by UV-Vis titration, and the binding constants (K_b) of the complexes were also calculated. The role of metal iridium in our complexes probably is to provide a coordination center, then the metal to ligand (MLCT) or ligand to metal charge transfer (LMCT) will appear, which can cause interaction between the complexes and ct-DNA via electrostatic or covalent action.^[12] As shown in **Figure 5** (**Figure S7** in supporting information) and **Table 3**, subtractive and small red shift ($\Delta\lambda = 6$ nm) along with the increase of

CT-DNA concentration indicate the interactions between complexes and DNA, which attributed to the interaction of complexes with base pairs in the form of electrostatic binding or noncovalent insertion.^[46] The binding constants K_b were fitted by Benesi–Hildebrand equation.^[12] As shown in **Table 3**, K_b will increase with the increase of the number of benzene rings on the Cp ring: $Cp^{xbiph} > Cp^{Xph} > Cp^*$. This result is in agreement with some previous studies.^[47]

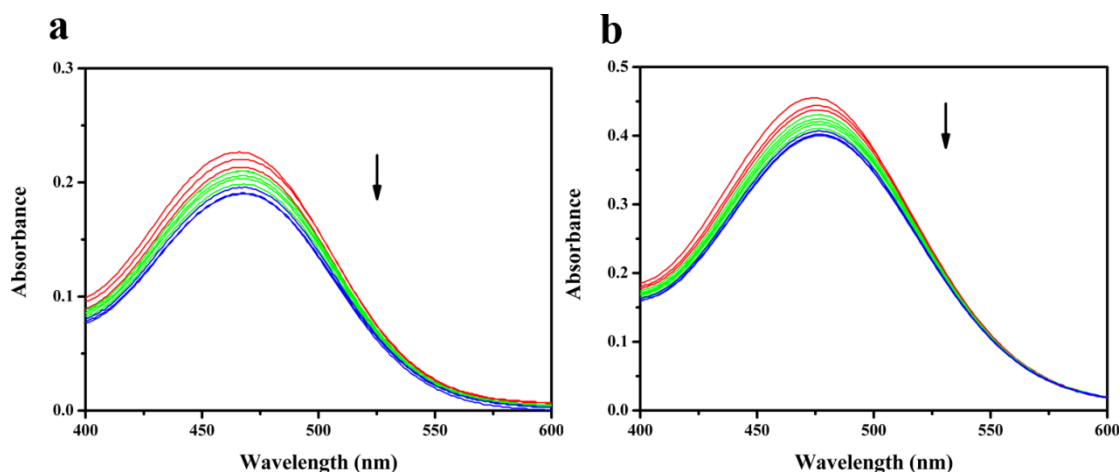


Figure 5 UV-Vis spectrum of complexes (a) **3** and (b) **6** dissolved in 10% DMSO 90% 5 mM Tris–HCl/50 mM NaCl buffer solution, pH = 7.2 (V:V) upon addition of the CT-DNA (0–0.4 mM) in 5 mM Tris–HCl/50 mM NaCl buffer solution (pH = 7.2). During the experiment, the concentration of the complexes remained unchanged and the concentration of CT-DNA increased continuously. The arrows show the direction of changes in absorbance upon increasing the concentration of CT-DNA.

Table 3 Absorption spectroscopic properties of as-synthesized complexes on binding to CT-DNA.

Complex	Absorption λ_{max} (nm)		$\Delta\lambda$	K_b (10^3 mM^{-1})
	Free	Bound ^a		
1	474	479	5	1.70
2	466	475	9	2.94
3	466	472	6	3.04
4	486	490	4	0.37
5	478	484	6	3.03
6	475	479	4	3.06

a: [Complex]=20 μM at [DNA]/[Complex]=20

2.5 Ethidium Bromide (EtBr) Displacement Studies

Ethidium bromide (EtBr) as an effective intercalation agent has a strong effect on nucleic acids and other biomolecules after dyeing, commonly used as fluorescent labeling of biological

molecules. EtBr itself has weak fluorescence, but the fluorescence intensity will increase about 20 times when it is combined with DNA into EtBr-DNA.^[31] As shown in **Figure 6** (**Figure S9** in supporting information), fluorescence quenching was found when adding the complexes **3** and **6** to a saturated EtBr-DNA solution. This phenomenon is attributed to the replacement of EtBr by Ir^{III} complexes from EtBr-DNA.^[48-52] The quenching relative to the initial intensity was 46% (**1**), 35% (**2**), 43% (**3**), 54% (**4**), 61% (**5**), and 65% (**6**), respectively. The quenching constants (K_q) are calculated by the Stern-Volmer equation,^[12] which were 1.13×10^4 (**1**), 1.32×10^4 (**2**), 2.50×10^4 (**3**), 2.11×10^4 (**4**), 3.82×10^4 (**5**), and 4.27×10^4 (**6**), respectively, which is consistent with the result of above CT-DNA binding test.

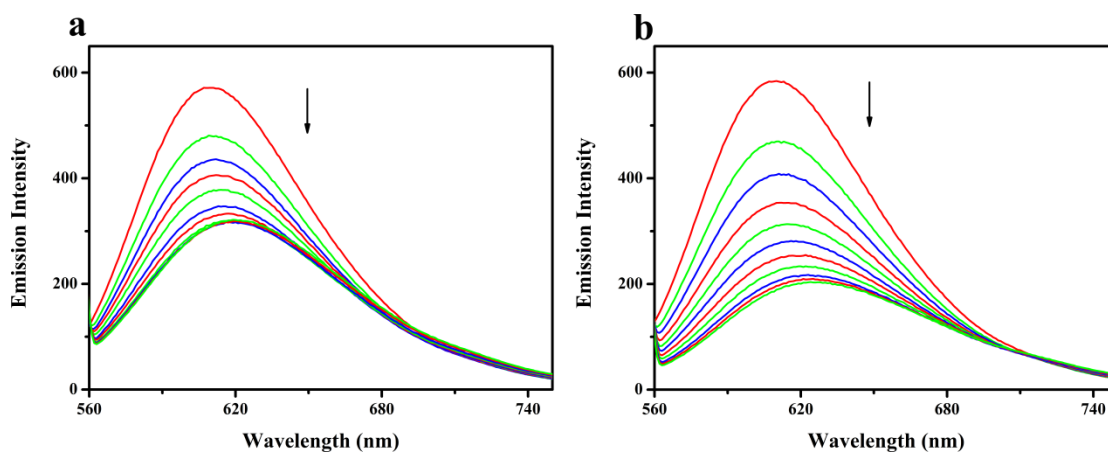


Figure 6 Fluorescence spectra of EtBr bound to DNA in the absence and presence of complexes (a) **3** and (b) **6** (0-50 μM dissolved in DMSO) (EtBr, 10 μM ; DNA, 10 μM ; in 5 mM Tris-HCl/50 mM NaCl buffer solution (pH = 7.2)). The arrows show changes in emission intensity upon increasing the amounts of complexes **3** and **6**.

As shown, the values of the binding constants K_q have a little change, the complexes with biphenyl rings on Cp ring have the strongest ability to replace EtBr compared to other complexes. The complexes may bind DNA via intercalation obtained from electronic absorption studies and the ability of the compound to bind to DNA increases with the increase of steric hindrance. From Cp* to Cp^{Xph} and Cp^{xbiph}, the binding features to BSA decrease, while to DNA increase, which could explain why complexes **2** and **4** showing the better anticancer activity.

2.6 Apoptosis Assay

In order to understand the function mechanism of complexes in cells, all complexes have analyzed apoptotic populations against A549 lung cancer cells by flow cytometry when exposure to as-synthesized complexes. As shown in **Figure 7** (**Table S2** and **S3**), flow cytometry analysis

showed that treatment of A549 cells with complexes 3 and 6 led to a dose-dependent increase in the percentage of apoptotic cells, respectively. After treatment for 24 h, when complex 3 at a concentration of $1 \times \text{IC}_{50}$, only 9.1% of A549 lung cancer cells were in late apoptotic phase. A total of 86.6% (early apoptotic + late apoptotic) cells were undergoing apoptosis at $3 \times \text{IC}_{50}$ for complex 3, whereas untreated cells remained 95.1% viable, indicating obvious induction of apoptosis at 3 equipotent concentrations of IC_{50} . For complex 6, 66.3% A549 lung cancer cells were in apoptotic phase at a concentration of $3 \times \text{IC}_{50}$.

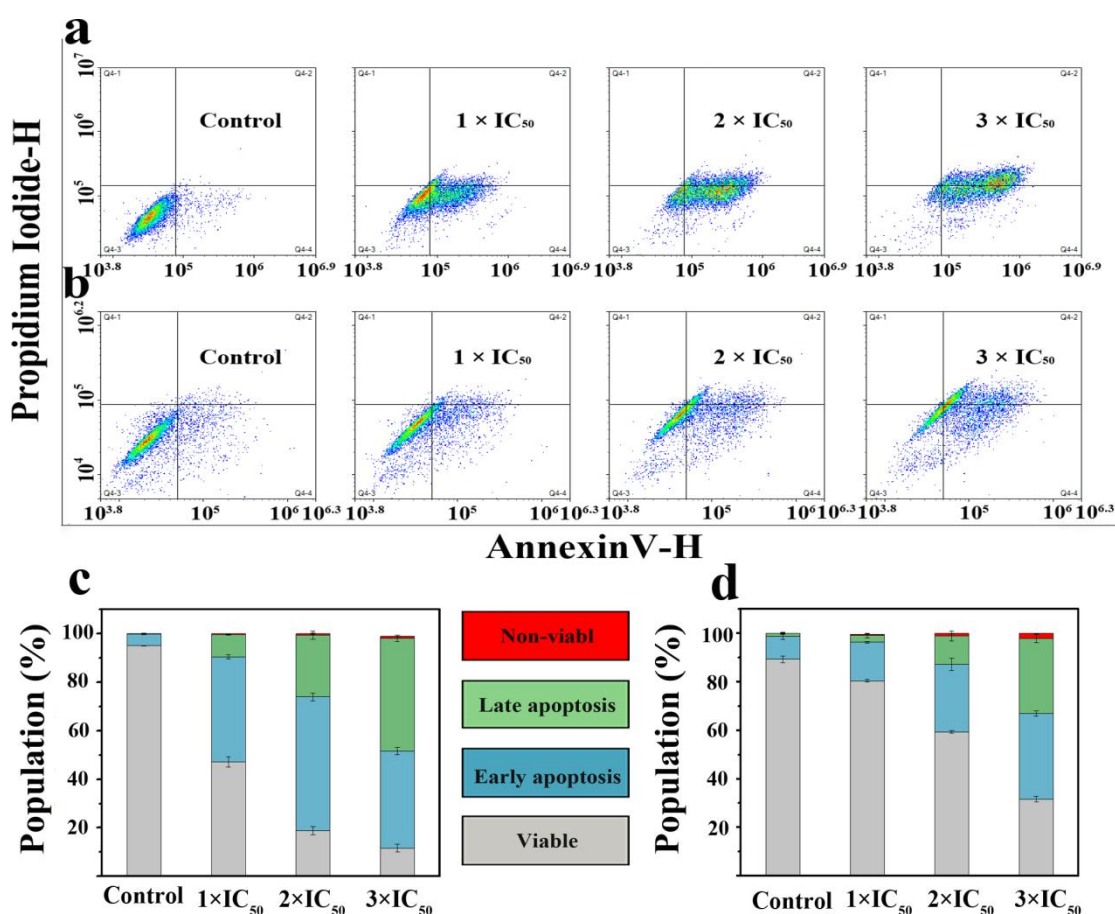


Figure 7 Apoptosis analysis of A549 lung cancer cells after 24 h of exposure to complexes (a) 3 and (b) 6 determined by flow cytometry using Annexin V-FITC vs PI staining. (c) 3 and (d) 6: Populations for cells treated by complexes 3 and 6, respectively.

2.7 Cell Cycle Analysis

Cell cycle arrest analysis for complexes 3 and 6 against A549 lung cancer cells investigated by flow cytometry was shown in **Figure 8** (Table S4 and S5). The cell cycle progression was analyzed at 0.25, 0.5 and 1 equipotent concentrations of IC_{50} of complexes for 24 h. At a concentration of $1 \times \text{IC}_{50}$, the percentages of cells in the S phase and G_1 phase increased 4% and 2%

when exposure to complex **3**. For complex **6**, at a concentration of $1 \times \text{IC}_{50}$, the percentages of cells in the G_2/M phase of the cell cycle increased from 8.9% to 10.2% and the Sub- G_1 phase increased from 0.1% to 1.8%. Compared with the untreated control, complex **3** disturbs the cell cycle at S phase, G_1 phase and Sub- G_1 phase, while complex **6** disturbing the cell cycle at S phase, G_2/M phase and Sub- G_1 phase. The results indicate that the complexes can disturb the cell growth cycle progression.

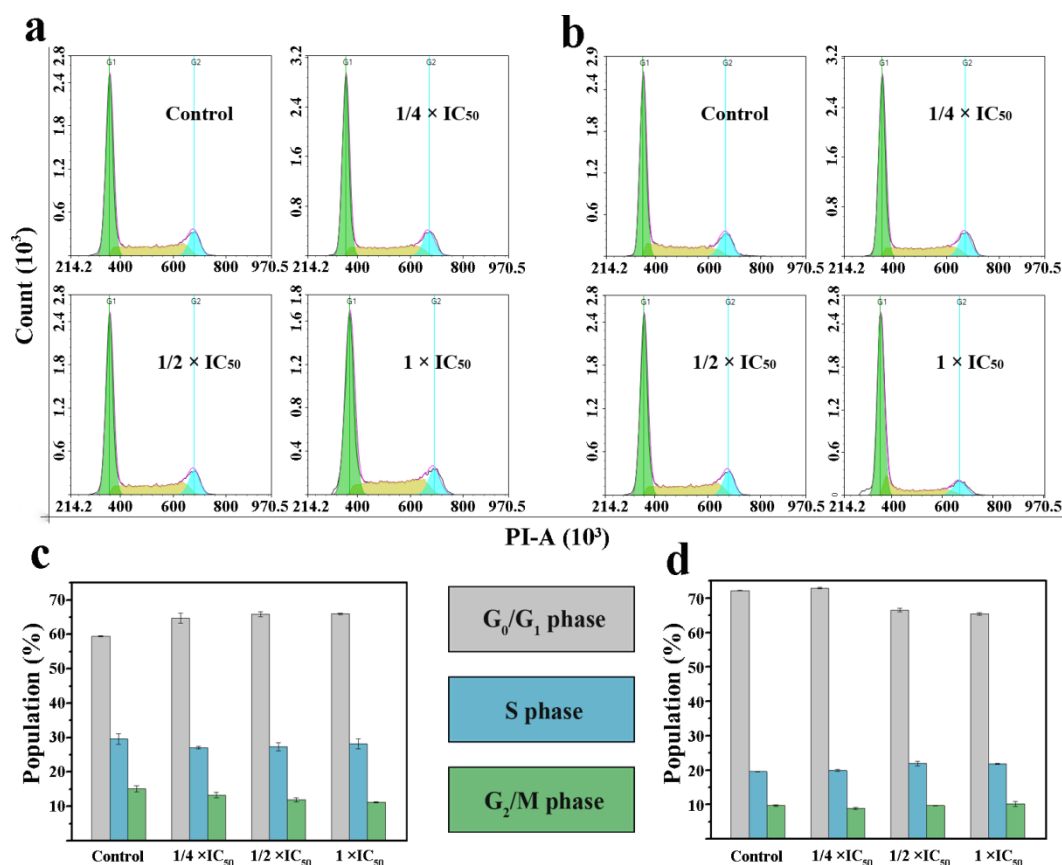


Figure 8 Cell cycle analysis of A549 lung cancer cells after 24 h of exposure to complexes (a) **3** and (b) **6** at the indicated concentrations by flow cytometry using PI staining. Populations in each cell cycle phase for control and complexes (c) **3** and (d) **6**.

2.8 Induction of ROS

Reactive oxygen species (ROS) plays an important role in regulating cell proliferation, death, and signaling, which is also used to explore the function mechanism of anticancer agents.^[15] The level of ROS in A549 lung cancer cells induced by complexes **3** and **6** at concentrations of $0.25 \times \text{IC}_{50}$ and $0.5 \times \text{IC}_{50}$ investigated by flow cytometry analysis. As shown in **Figure 9** (Table S6 and S7), treatment with complexes **3** and **6** after 24 h, the increasing of ROS levels at A549 lung cancer cells were observed. The changes of ROS level have provided a basis for killing cancer

cells.^[16]

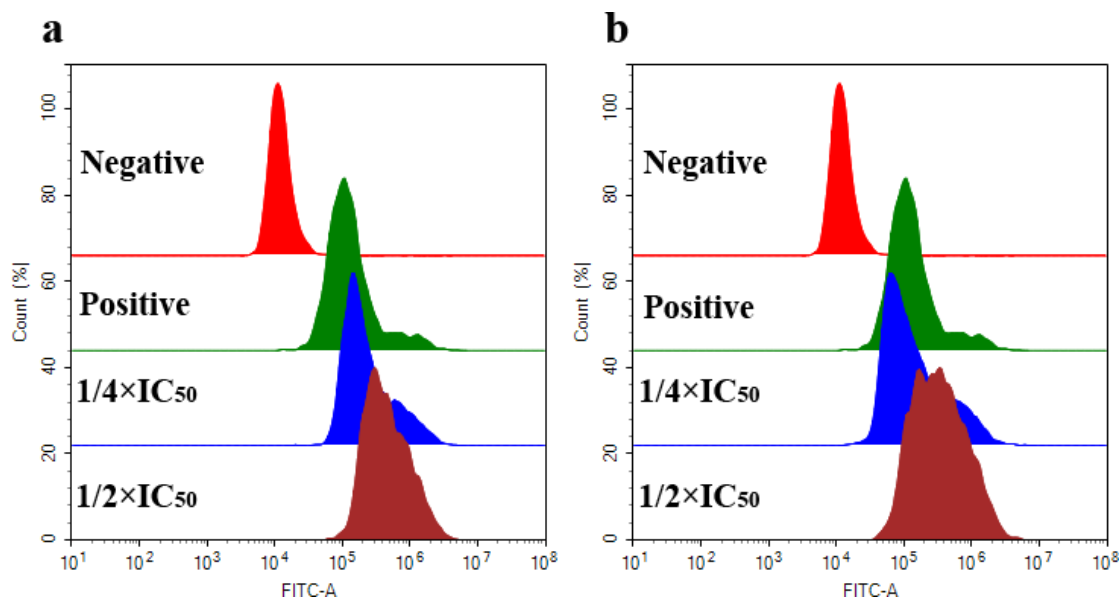


Figure 9 Effect of complexes (a) **3** and (b) **6** on intracellular ROS levels in A549 lung cancer cells treated at the indicated concentrations for 24 h.

CONCLUSION

In this study, six new half-sandwich Ir^{III} complexes were synthesized with simple synthetic procedures. The introduction of TPA group to bipyridine ligand has effectively improved the anticancer activity of complexes. Complex **2** showed the best activity towards A549 lung cancer cells (IC₅₀: 1.5 μM), which was more than ten times higher than the clinical anticancer drug *cis*-platin. From Cp^{*} to Cp^{Xph} and Cp^{xbiph}, the binding features to BSA decrease, while to DNA increase, which further verifies why complexes **2** and **4** showing the better anticancer activity. And also, Ir^{III} complexes can induce ROS in cells, which can lead to apoptosis. The results of flow cytometry further indicate that the complexes can disturb the cell growth cycle and lead to apoptosis. Above all, triphenylamine-appended half-sandwich iridium^{III} complexes could be a promising candidate for further evaluation as anti-cancer drugs.

EXPERIMENTAL SECTION

Materials

IrCl₃ · nH₂O, 4-(di-*p*-tolylamino)benzaldehyde, 4-(bis(4-methoxyphenyl)amino)benzaldehyde, 2,3,4,5-tetramethyl-2-cyclopentenone(95%), 1,2,3,4,5-pentamethyl-cyclopentadiene(95%), butyllithium solution (1.6 M in hexane), 4'-methyl-[2,2'-bipyridine]-4-carbaldehyde, 4-(di-*p*-tolyla

mino)benzaldehyde, 4-(bis(4-methoxyphenyl)amino)benzaldehyde and (λ^2 -bromanyl)triphenyl- λ^4 -phosphane were purchased from Shanghai Pengteng Fine Chemical Co., Ltd. For the biological experiments, DMEM medium, fetal bovine serum, penicillin/streptomycin mixture and trypsin/EDTA were purchased from Sangon Biotech. A549 lung cancer cells were obtained from Shanghai Institute of Biochemistry and Cell Biology (SIBCB).

Syntheses

Synthesis of Wittig reagents (**F**)

The intermediates (**D**) and Wittig reagents (**F**) were synthesized according to the literature.^[53]

Synthesis of ligand (**L**).^[54,55]

Wittig reagents **F** (3 mmol) and 4'-methyl-[2,2'-bipyridine]-4-carbaldehyde (1.5 mmol) were added into a 100 mL round-bottom flask under N_2 . Anhydrous THF (40 mL) was added to above flask, cooled down to 0 °C. The THF solution of t-BuOK (3 mmol,) was added dropwise to above flask, stirred for 30 min at 0 °C, followed by stirring at room temperature until Wittig reagents **F** was consumed completely (monitored by thin-layer chromatography). The reaction was terminated with ice water. The crude product was refluxed for 8 h in THF with a catalytic amount of iodine. Then the remaining iodine was removed by sodium hydroxide (NaOH) solution (Wt = 10%, 100 mL) with stirring for 2 h. After that, the product was purified by chromatographed on a silica gel column (petroleum ether: ethyl acetate =15:1 as eluent) to give the title complexes as a pure *E* stereoisomer.

(E)-4-methyl-N-(4-(2-(4'-methyl-[2,2'-bipyridin]-4-yl)vinyl)phenyl)-N-(p-tolyl)aniline

(L1): Yield: 2.9 g (51.6%). ¹H NMR (500 MHz, CDCl₃) δ 8.60 (dt, *J* = 15.7, 8.0 Hz, 2H), 7.42 – 7.35 (m, 4H), 7.14 – 7.08 (m, 4H), 7.04 – 6.79 (m, 10H), 3.83 (s, 6H), 2.49 (s, 3H).

(E)-4-methoxy-N-(4-methoxyphenyl)-N-(4-(2-(4'-methyl-[2,2'-bipyridin]-4-yl)vinyl)phenyl)anilin (L2): Yield: 2.8 g (49.6%). ¹H NMR (500 MHz, CDCl₃) δ 8.62 – 8.55 (m, 2H), 8.48 (s, 1H), 8.26 (s, 1H), 7.43 – 7.32 (m, 4H), 7.14 (t, *J* = 6.3 Hz, 1H), 7.09 (d, *J* = 8.2 Hz, 4H), 7.04 – 6.94 (m, 7H), 2.45 (s, 3H), 2.33 (s, 6H).

Synthesis of the $[(\eta^5\text{-C}_5\text{Me}_5)\text{IrCl}_2]_2$ (**dimer1**), $[(\eta^5\text{-C}_5\text{Me}_4\text{C}_6\text{H}_5)\text{IrCl}_2]_2$ (**dimer2**) and $[(\eta^5\text{-C}_5\text{Me}_4\text{C}_6\text{H}_4\text{C}_6\text{H}_5)\text{IrCl}_2]_2$ (**dimer3**).

Dimers were prepared according to literature methods.^[18]

$[(\eta^5\text{-C}_5\text{Me}_5)\text{IrCl}_2]_2$ (**dimer1**): Yield: 0.397 g (64.6%). ¹H NMR (500 MHz, CDCl₃): δ 1.60 (s,

$J = 1.4$ Hz, 15H).

$[(\eta^5\text{-C}_5\text{Me}_4\text{C}_6\text{H}_5)\text{IrCl}_2]_2$ (**dimer2**): Yield: 0.37 g (58.5%). $^1\text{H NMR}$ (500 MHz, CDCl_3): δ 7.58 (m, 2H), 7.35 (m, 3H), 1.72 (s, 6H), 1.63 (s, 6H).

$[(\eta^5\text{-C}_5\text{Me}_4\text{C}_6\text{H}_4\text{C}_6\text{H}_5)\text{IrCl}_2]_2$ (**dimer3**): Yield: 0.25 g (35.8%). $^1\text{H NMR}$ (500 MHz, CDCl_3): δ 7.64 (m, 4H), 7.44 (m, 2H), 7.33 (m, 3H), 3.25 (m, 1H), 2.08 (s, 3H), 1.95 (s, 3H), 1.88 (s, 3H), 1.00 (d, 3H, $J = 7.5$ Hz).

Synthesis of the $[(\eta^5\text{-Cp}^x)\text{Ir}(\text{N}^{\wedge}\text{N})\text{Cl}]\text{PF}_6$.

A solution of $[(\eta^5\text{-Cp}^x)\text{IrCl}_2]_2$ (0.05 mmol) and complexes L (0.1 mmol) in methanol (40 mL) resulting suspension was stirred at ambient temperature overnight. The mixture was then stirred with addition of ammonium hexafluorophosphate (0.4mmol) for 4h. Most of the solvent is concentrated in vacuum and kept at -20 °C for 12h, filtered and washed with cold methanol and diethyl ether. The $^1\text{H NMR}$ (500 MHz, CD_3Cl_3) peak integrals of complexes **1-6** are shown in (**Figure S11** in supporting information). The high resolution mass spectrometry data of complexes **1-6** are shown in (**Figure S12** in supporting information).

$[(\eta^5\text{-Cp}^x)\text{Ir}(\text{N}^{\wedge}\text{N})\text{Cl}]\text{PF}_6$ (**1**). Yield: 0.032 g (35.8%). $^1\text{H NMR}$ (500 MHz, CDCl_3): δ 8.54 (d, $J = 5.8$ Hz, 1H), 8.50 (d, $J = 6.0$ Hz, 1H), 8.32 (d, $J = 16.7$ Hz, 2H), 7.58 (d, $J = 5.9$ Hz, 1H), 7.53 (d, $J = 16.2$ Hz, 1H), 7.44 (d, $J = 8.8$ Hz, 3H), 7.11 (d, $J = 8.2$ Hz, 4H), 7.04 (d, $J = 8.3$ Hz, 4H), 6.99 – 6.94 (t, 3H), 2.62 (s, 3H), 2.34 (s, 6H), 1.66 (s, 15H). ESI-MS (m/z): $[\text{M-PF}_6]^+$ Calcd for $\text{C}_{43}\text{H}_{44}\text{ClIrN}_3$, 830.513; Found 830.863. $[\text{M-PF}_6\text{-Cl}]^+$ Calcd for $\text{C}_{43}\text{H}_{44}\text{IrN}_3$, 795.063; Found 794.926. Elemental analysis: Found: C, 52.89; H, 4.53; N, 4.32%, calcd for $\text{C}_{43}\text{H}_{44}\text{ClF}_6\text{IrN}_3\text{P}$: C, 52.95; H, 4.55; N, 4.31%.

$[(\eta^5\text{-Cp}^x)\text{Ir}(\text{N}^{\wedge}\text{N})\text{Cl}]\text{PF}_6$ (**2**). Yield: 0.025 g (30.2%). $^1\text{H NMR}$ (500 MHz, CDCl_3): δ 8.37 (dd, $J = 16.5, 9.1$ Hz, 3H), 8.30 (d, $J = 6.1$ Hz, 1H), 7.60 – 7.41 (m, 10H), 7.34 (d, $J = 5.2$ Hz, 1H), 7.10 (d, $J = 8.3$ Hz, 4H), 7.03 (d, $J = 8.3$ Hz, 4H), 6.95 (d, $J = 8.6$ Hz, 2H), 2.64 (s, 3H), 2.33 (s, 6H), 1.76 (d, $J = 3.1$ Hz, 6H), 1.72 (s, 6H). ESI-MS (m/z): $[\text{M-PF}_6]^+$ Calcd for $\text{C}_{48}\text{H}_{46}\text{ClIrN}_3$, 892.584; Found 892.884. $[\text{M-PF}_6\text{-Cl}]^+$ Calcd for $\text{C}_{48}\text{H}_{46}\text{IrN}_3$, 857.134; Found 856.909. Elemental analysis: Found: C, 55.47; H, 4.43; N, 4.04%, calcd for $\text{C}_{48}\text{H}_{46}\text{ClF}_6\text{IrN}_3\text{P}$: C, 55.57; H, 4.47; N, 4.05%.

$[(\eta^5\text{-Cp}^x)\text{Ir}(\text{N}^{\wedge}\text{N})\text{Cl}]\text{PF}_6$ (**3**). Yield: 0.040 g (43.2%). $^1\text{H NMR}$ (500 MHz, CDCl_3): δ 8.40 (dd, $J = 7.5, 4.3$ Hz, 3H), 8.34 (d, $J = 6.1$ Hz, 1H), 7.74 (d, $J = 8.3$ Hz, 2H), 7.69 – 7.63 (m, 4H),

7.55 (s, 1H), 7.53 – 7.47 (m, 3H), 7.47 – 7.42 (m, 3H), 7.37 (d, $J = 5.7$ Hz, 1H), 7.11 (d, $J = 8.2$ Hz, 3H), 7.07 (d, $J = 8.6$ Hz, 1H), 7.03 (d, $J = 8.3$ Hz, 3H), 7.00 (d, $J = 4.8$ Hz, 1H), 6.96 (d, $J = 8.9$ Hz, 2H), 6.89 (d, $J = 8.6$ Hz, 1H), 2.68 (s, 3H), 2.32 (d, $J = 10.3$ Hz, 6H), 1.78 (m, $J = 12.2$, 6.1 Hz, 12H). ESI-MS (m/z): $[M-PF_6]^+$ Calcd for $C_{54}H_{50}ClIrN_3$, 968.682; Found 968.145. $[M-PF_6-Cl]^+$ Calcd for $C_{54}H_{50}IrN_3$, 933.282; Found 933.183. Elemental analysis: Found: C, 58.13; H, 4.50; N, 3.78%, calcd for $C_{54}H_{50}ClF_6IrN_3P$: C, 58.24; H, 4.53; N, 3.77%.

$[(\eta^5-Cp^x)Ir(N^{\wedge}N)Cl]PF_6$ (**4**). Yield: 0.033 g (36.5%). 1H NMR (500 MHz, $CDCl_3$): 8.47 (d, $J = 5.8$ Hz, 1H), 8.42 (d, $J = 6.1$ Hz, 1H), 8.25 (d, $J = 12.5$ Hz, 2H), 7.48 (dd, $J = 22.5$, 10.8 Hz, 2H), 7.40 – 7.30 (t, 3H), 7.01 (d, $J = 13.3$ Hz, 4H), 6.84 (dd, $J = 35.5$, 12.2 Hz, 7H), 3.75 (s, 6H), 2.55 (s, 3H), 1.59 (s, 15H). ESI-MS (m/z): $[M-PF_6]^+$ Calcd for $C_{48}H_{46}ClIrN_3O_2$, 862.275; Found 862.103 $[M-PF_6-Cl]^+$ Calcd for $C_{48}H_{46}IrN_3O_2$, 827.061; Found 827.141. Elemental analysis: Found: C, 51.16; H, 4.42; N, 4.19%, calcd for $C_{43}H_{44}ClF_6IrN_3O_2P$: C, 51.26; H, 4.40; N, 4.17%.

$[(\eta^5-Cp^x)Ir(N^{\wedge}N)Cl]PF_6$ (**5**). Yield: 0.036 g (38.3%). 1H NMR (500 MHz, $CDCl_3$): δ 8.37 (dd, $J = 14.1$, 7.4 Hz, 3H), 8.29 (d, $J = 6.1$ Hz, 1H), 7.59 – 7.39 (m, 10H), 7.33 (d, $J = 5.3$ Hz, 1H), 7.09 (d, $J = 8.8$ Hz, 4H), 6.86 (d, $J = 8.9$ Hz, 6H), 3.81 (s, 6H), 2.63 (s, 3H), 1.76 (d, $J = 3.5$ Hz, 6H), 1.71 (s, 6H). ESI-MS (m/z): $[M-PF_6]^+$ Calcd for $C_{43}H_{44}ClIrN_3O_2$, 924.582; Found 924.705 $[M-PF_6-Cl]^+$ Calcd for $C_{43}H_{44}IrN_3O_2$, 889.132; Found 889.533. Elemental analysis: Found: C, 53.82; H, 4.32; N, 3.94%, calcd for $C_{48}H_{46}ClF_6IrN_3O_2P$: C, 53.90; H, 4.34; N, 3.93%.

$[(\eta^5-Cp^x)Ir(N^{\wedge}N)Cl]PF_6$ (**6**). Yield: 0.05 g (52.1%). 1H NMR (500 MHz, $CDCl_3$) δ 8.42 – 8.38 (m, 3H), 8.32 (d, $J = 6.1$ Hz, 1H), 7.73 (d, $J = 8.3$ Hz, 2H), 7.66 (dd, $J = 12.4$, 8.3 Hz, 4H), 7.55 – 7.46 (m, 4H), 7.43 (t, $J = 8.8$ Hz, 3H), 7.36 (d, $J = 6.1$ Hz, 1H), 7.09 (d, $J = 8.9$ Hz, 4H), 6.96 (d, $J = 16.1$ Hz, 1H), 6.89 – 6.84 (m, 6H), 3.81 (s, 6H), 2.66 (s, 3H), 1.82 – 1.73 (m, 12H). ESI-MS (m/z): $[M-PF_6]^+$ Calcd for $C_{54}H_{50}ClIrN_3O_2$, 1000.680; Found 1000.856. $[M-PF_6-Cl]^+$ Calcd for $C_{54}H_{50}IrN_3O_2$, 963.351; Found 963.902. Elemental analysis: Found: C, 56.52; H, 4.38; N, 3.64%, calcd for $C_{54}H_{50}ClF_6IrN_3O_2P$: C, 56.61; H, 4.40; N, 3.67%.

ACKNOWLEDGMENTS

We thank the National Natural Science Foundation of China (Grant No. 21671118) and the Taishan Scholars Program for support.

Notes

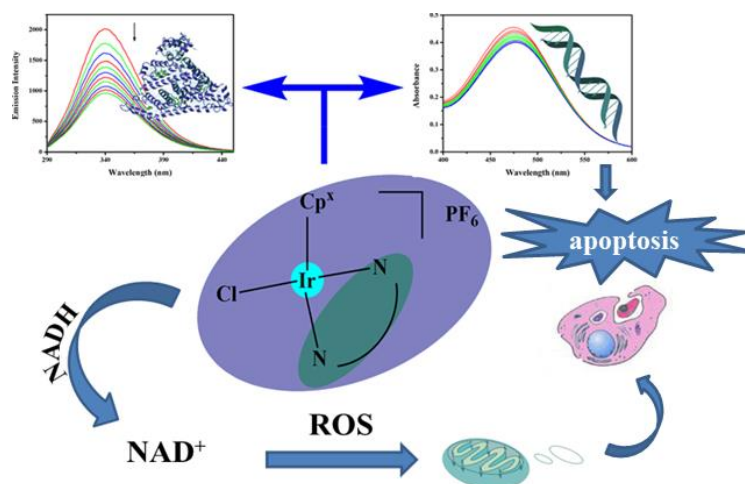
The authors declare no competing financial interest.

References

- [1] G. Gasser, I. Ott, N. Metzlerolte, *J. Med. Chem.* **2011**, *54*, 3-25.
- [2] P. Zhang, P.J. Sadler, *J. Organomet. Chem.* **2017**, *839*, 5-14.
- [3] Z. Liu, P.J. Sadler, *Acc. Chem. Res.* **2014**, *47*, 1174-1185.
- [4] Y. Li, C.P. Tan, W. Zhang, L. He, L.N. Ji, Z.W. Mao, *Biomaterials.* **2015**, *39*, 95-104.
- [5] C.H. Leung, H.J. Zhong, S.H. Chan, D.L. Ma, *Coord. Chem. Rev.* **2013**, *257*, 1764-1776.
- [6] P.K. Sasmal, C.N. Streu, E. Meggers, *Chem. Commun.* **2013**, *49*, 1581-1587.
- [7] N. Cutillas, G.S. Yellol, C.D. Haro, C. Vicente, V. Rodríguez, J. Ruiz, *Coord. Chem. Rev.* **2013**, *257*, 2784-2797
- [8] L. He, Y. Li, C. Tan, R.R. Ye, M.H. Chen, J.J. Cao, L.N. Ji, Z.W. Mao, *Chem. Sci.* **2015**, *6*, 5409-5418.
- [9] R.R. Ye, C.P. Tan, L. He, M.H. Chen, L.N. Ji, Z.W. Mao, *Chem. Commun.* **2014**, *50*, 10945-10948.
- [10] Š. P, A. Habtemariam, I. Romerocanelón, G.J. Clarkson, P.J. Sadler, *Inorg. Chem.* **2016**, *4*, 23-39.
- [11] L. Tabrizi, H. Chiniforoshan, *Dalton. Trans.* **2017**, *46*, 2339.
- [12] S. Mukhopadhyay, R.K. Gupta, R.P. Paitandi, N.K. Rana, G. Sharma, B. Koch, L.K. Rana, M.S. Hundal, D.S. Pandey, *Organometallics.* **2015**, *34*, 4491-4506.
- [13] L. Tabrizi, H. Chiniforoshan, *Dalton. Trans.* **2017**, *46*, 2339-2349.
- [14] Y. Zheng, L. He, D.Y. Zhang, C.P. Tan, L.N. Ji, Z.W. Mao, *Dalton. Trans.* **2017**, *46*, 11395-11407
- [15] Z. Liu, I. Romerocanelón, B. Qamar, J.M. Hearn, A. Habtemariam, N.P. Barry, A.M. Pizarro, G.J. Clarkson, P.J. Sadler, *Angew. Chem. Int. Ed.* **2014**, *53*, 3941-3946.
- [16] J.M. Hearn, I. Romerocanelon, B. Qamar, Z. Liu, I. Handsportman, P.J. Sadler, *ACS. Chem. Biol.* **2013**, *8*, 1335-1343.
- [17] V. Novohradsky, L. Zerzankova, J. Stepankova, A. Kisova, H. Kostrhunova, Z. Liu, P.J. Sadler, J. Kasparkova, V. Brabec, *Metallomics.* **2014**, *6*, 1491-1501.
- [18] C. Wang, J. Liu, Z. Tian, M. Tian, L. Tian, W. Zhao, Z. Liu, *Dalton. Trans.* **2017**, *46*, 6870-6883.
- [19] L. He, C.P. Tan, R.R. Ye, Y.Z. Zhao, Y.H. Liu, Q. Zhao, L.N. Ji, Z.W. Mao, *Angew. Chem. Int. Ed.* **2014**, *53*, 12137-12141.
- [20] J. Li, M. Tian, Z. Tian, S. Zhang, C. Yan, C. Shao, Z. Liu, *Inorg. Chem.* **2018**, *57*, 1705-1716.
- [21] Z. Liu, P.J. Sadler, *Acc. Chem. Res.* **2014**, *47*, 1174-1185.
- [22] Z. Liu, A. Habtemariam, A.M. Pizarro, S.A. Fletcher, A. Kisova, O. Vrana, L. Salassa, P.C.A. Bruijninx, G.J. Clarkson, V. Brabec, *J. Med. Chem.* **2011**, *54*, 3011-3026.
- [23] Y. Li, B. Liu, X.R. Lu, M.F. Li, L.N. Ji, Z.W. Mao, *Dalton. Trans.* **2017**, *46*, 11363-11371.
- [24] Š. P, A. Habtemariam, I. Romero-Canelón, G.J. Clarkson, P.J. Sadler, *Inorg. Chem.* **2016**, *4*, 23-39.
- [25] V. Novohradsky, Z. Liu, M. Vojtiskova, P.J. Sadler, V. Brabec, J. Kasparkova, *Metallomics.* **2014**, *6*, 682-690.
- [26] Z. Liu, R.J. Deeth, J.S. Butler, H. Abraha, M.E. Newton, P.J. Sadler, *Angew. Chem. Int. Ed.* **2013**, *52*, 4194-4197.
- [27] B.L. Soledad, L. Zhe, H. Abraha, A.M. Pizarro, Q. Bushra, P.J. Sadler, *Angew. Chem. Int. Ed.* **2012**, *124*, 3963-3966.

- [28] R. Esteghamat-Panah, H. Hadadzadeh, H. Farrokhpour, M. Mortazavi, Z. Amirghofran, *Inorg. Chim. Acta.* **2016**, *454*, 184-196.
- [29] B.K. Paul, K. Bhattacharjee, S. Bose, N. Guchhait, *Phys. Chem. Chem. Phys.* **2012**, *14*, 15482-15493.
- [30] C. Umadevi, P. Kalaivani, H. Puschmann, S. Murugan, P.S. Mohan, R. Prabhakaran, *J. Photochem. Photobiol. B.* **2017**, *167*, 45-57.
- [31] Y.J. Wang, R.D. Hu, D.H. Jiang, P.H. Zhang, Q.Y. Lin, Y.Y. Wang, *J. Fluoresc.* **2011**, *21*, 813-823.
- [32] O. Dömötör, C.G. Hartinger, A.K. Bytzeck, T. Kiss, B.K. Keppler, E.A. Enyedy, *Biol. Inorg. Chem.* **2013**, *18*, 9-17.
- [33] R.D. Senthil, N.S. Bhuvanesh, K. Natarajan, *Eur. J. Med. Chem.* **2011**, *46*, 4584-4594.
- [34] D.S. Raja, G. Paramaguru, N.S. Bhuvanesh, J.H. Reibenspies, R. Renganathan, K. Natarajan, *Dalton. Trans.* **2011**, *40*, 4548-4559.
- [35] M.R. Eftink, C.A. Ghiron, *J. phys. chem.* **1976**, *80*, 486-493.
- [36] R. Pettinari, F. Marchetti, A. Petrini, C. Pettinari, G. Lupidi, B. Fernández, A.R. Diéguez, G. Santoni, M. Nabissi, *Inorg. Chim. Acta.* **2016**, *454*, 139-148.
- [37] E. Ramachandran, R.D. Senthil, N.S. Bhuvanesh, K. Natarajan, *Dalton. Trans.* **2012**, *41*, 13308-13323.
- [38] D.S. Raja, N.S. Bhuvanesh, K. Natarajan, *Dalton. Trans.* **2012**, *41*, 4365-4377.
- [39] Z. Chen, J. Zhang, C. Liu, *BioMetals.* **2013**, *26*, 827-838.
- [40] Y.Z. Zhang, B. Zhou, Y.X. Liu, C.X. Zhou, X.L. Ding, Y. Liu, *J. Fluoresc.* **2008**, *18*, 109-118.
- [41] J. Tang, F. Luan, X. Chen, *Bioorg. Med. Chem.* **2006**, *14*, 3210-3217.
- [42] J. Li, L. Guo, Z. Tian, M. Tian, S. Zhang, K. Xu, Y. Qian, Z. Liu, *Dalton. Trans.* **2017**, *46*, 15520-15534.
- [43] Roberta Cacciapaglia, Alessandro Casnati, Luigi Mandolini, †, A. Peracchi, D.N.R. §, ,, Riccardo Salvio, A. *J. Am. Chem. Soc.* **2007**, *129*, 12512-12520.
- [44] L. Tjioe, A. Meininger, T. Joshi, L. Spiccia, B. Graham, *Inorg. Chem.* **2011**, *50*, 4327-4339.
- [45] M. Tian, J. Li, S. Zhang, L. Guo, X. He, D. Kong, H. Zhang, Z. Liu, *Chem. Commun.* **2017**, *53*, 12810-12813.
- [46] L.-J. Li, B. Fu, Y. Qiao, C. Wang, Y.-Y. Huang, C.-C. Liu, C. Tian, J.-L. Du, *Inorg. Chim. Acta.* **2014**, *419*, 135-140.
- [48] B. Maity, M. Roy, B. Banik, R. Majumdar, R.R. Dighe, A.R. Chakravarty, *Organometallics.* **2010**, *29*, 3632-3641.
- [49] E.C. Long, J.K. Barton, *Acc. Chem. Res.* **1990**, *23*, 271-273.
- [50] R.F. Pasternack, E.J. Gibbs, J.J. Villafranca, *Biochem. Anal. Biochem.* **1983**, *22*, 5409-5417.
- [51] Z.C. Liu, B.D. Wang, Z.Y. Yang, Y. Li, D.D. Qin, T.R. Li, *Eur. J. Med. Chem.* **2009**, *44*, 4477-4484.
- [52] Z. Atay, T. Biver, A. Corti, N. Eltugral, E. Lorenzini, M. Masini, A. Paolicchi, A. Pucci, G. Ruggeri, F. Secco, *J. Nanopart. Res.* **2010**, *12*, 2241-2253.
- [53] M. Howegrant, K.C. Wu, W.R. Bauer, S.J. Lippard, *Biochem. Anal. Biochem.* **1976**, *15*, 4339-4346.
- [54] X. Liu, F. Zhang, Z. Liu, Y. Xiao, S. Wang, X. Li, *J. Mater. Chem. C.* **2017**, *5*, 11429 - 11435
- [55] X. Liu, L. Zhu, F. Zhang, J. You, Y. Xiao, D. Li, S. Wang, Q. Meng, X. Li, *Energy. Technol.* **2017**, *5*, 312-330.
- [56] X. Liu, J. You, Y. Xiao, S. Wang, W. Gao, J. Peng, X. Li, *Dyes. Pigm.* **2016**, *125*, 36-43.

Table-of-Contents



Organometallic half-sandwich Ir^{III} complexes of type $[(\eta^5\text{-Cp}^x)\text{Ir}(\text{N}^1\text{N})\text{Cl}]\text{PF}_6$ (N^1N : triphenylamine substituted bipyridyl ligand) showed potent cytotoxicity and excellent BSA and DNA binding properties, and catalytic conversion of NADH to NAD⁺. The complexes significantly increased reactive oxygen species (ROS) in cells and induced apoptosis effectively.